J Mol Model (2012) 18:3793–3804
DOI 10.1007/s00894-012-1371-x

ORIGINAL PAPER

Selective oxidation of propylamine on oxygen-covered Au(111): a DFT study

Xian-Yong Pang · Juan-Juan Wang · Gui-Chang Wang

Received: 15 December 2011 / Accepted: 30 January 2012 / Published online: 7 March 2012
© Springer-Verlag 2012

Abstract The reaction mechanism for selective oxidation of propylamine on oxygen-covered gold has been studied by the density functional theory (DFT) and generalized gradient approximation (GGA) with slab model. Our calculation results indicated that the adsorption energy of propylamine decreases with the increasing oxygen coverage, that is −0.38, −0.20 and −0.10 eV on clean, 2/9 monolayer (ML) and 2/3 monolayer (ML) oxygen, respectively. The adsorption energies of the intermediates also have the trend of the gradual lower. The present work also indicated that the final product distribution depends on the oxygen coverage: propylamine undergoes N-H bond and C-H bond cleavage to produce propionitrile and water at low-oxygen-coverage (θ_o=2/9 ML), and to yield propionitrile, propionaldehyde and water at high-oxygen-coverage (θ_o=2/3 ML). The energy barrier of the first step of propyamine oxidation ($CH_3CH_2CH_2NH_2 \rightarrow CH_3CH_2CH_2NH$) is 0.16 eV ($\theta_o$=2/9 ML) and 0.38 eV ($\theta_o$=2/3 ML). On the second step, the barrier energy is 0.16 (θ_o=2/9 ML) and 0.25 (θ_o=2/3 ML) eV of $CH_3CH_2CH_2NH \rightarrow CH_3CH_2CH_2N$, next both C-H breakage and the barrier energy is 0.20 eV ($CH_3CH_2CH_2N \rightarrow CH_3CH_2CHN$) and 0.25 eV ($CH_3CH_2CHN \rightarrow CH_3CH_2CN$) on low oxygen coverage, and 0.15 eV ($CH_3CH_2CH_2N \rightarrow CH_3CH_2CHN$) and 0.26 eV ($CH_3CH_2CHN \rightarrow CH_3CH_2CN$) on the high oxygen coverage. The additional reaction step of $CH_3CH_2CHN \rightarrow CH_3CH_2CHO$ occurs on the high oxygen coverage, and the associated barrier is 0.41 eV. The calculation results show that the oxidation of propylamine can occur at room temperature due to the lower energy barrier. Furthermore, it was found that the energy barrier for the possible reaction steps at the low oxygen coverage is generally smaller than that on high oxygen coverage, which agrees with the experimental results.

Keywords Au(111) · DFT calculation · Oxygen coverage effect · Propylamine · Selective oxidation

X.-Y. Pang · J.-J. Wang
College of Chemistry and Chemical Engineering,
Taiyuan University of Technology,
Taiyuan 030024, People's Republic of China

X.-Y. Pang
e-mail: pangxy_tyut@126.com

G.-C. Wang
Department of Chemistry, Nankai University,
Tianjin 300071, People's Republic of China

G.-C. Wang (✉)
College of Chemistry and Chemical Engineering,
Shanxi Datong University,
Datong 037009, Shanxi Province, People's Republic of China
e-mail: wangguichang@nankai.edu.cn

Introduction

Due to environmental pollution, pollution-free, cleaning pollution and disposal of chemical contaminants is particularly important [1, 2]. Research on ways to clean the polluted air becomes more and more important. For removing ammonia from NHx-containing waste gases, a perfect method is selective catalytic oxidation of ammonia to produce nitrogen and water [3, 4]. Because amine is indispensable in many heterogeneously catalytic process, and thus amine and amine derivatives have been widely investigated. The basic amine group is frequently chosen as reactants, products and catalyst modifiers [5, 6], and receives a great deal of interest. Garden et al. [5] demonstrated that understanding the feature of adsorbed organic nitrogen molecules and a series of their reactions on metal surfaces is important for further understanding the detailed reaction mechanism including the breakage of C–H、N–H and C–N bonds.

Gold is usually regarded as the chemical inertness; however, the extensive experimental results showed that the oxygen pre-covered gold can catalyze many reactions, which shows that the surface of gold is not completely inert [7]. Because it is a benefit for developing environmentally benign processes, now people pay more attention on the golden heterogeneous catalysis [8, 9]. Au-based system is considered as a good model surface, because the highly dispersed gold nanoparticles supported on oxides possess unique catalytic activity [10]. At low temperature, metal-oxide supported gold nanoparticles can be used to active CO and propylene [11]. More attention is paid to gold, which is highly active for selective hydrogenation, selective oxidation of ammonia and epoxidation of propylene [3, 12, 13]. Moreover, numerous experimental studies demonstrated that the gold particles are active for the oxidation of amines [10, 14, 15]. More recently Gong et al. [15] studied the oxidation of propylamine on the oxygen-adsorbed Au (111), in which they found that final products distribution strongly depends on the oxygen coverage. At low oxygen coverage (θ_O<0.5 ML) propylamine ($CH_3CH_2CH_2NH_2$) undergoes N-H and C-H bond breaking to produce propionitrile (CH_3CH_2CN) and water (H_2O), while the formation of propionitrile, propaldehyde (CH_3CH_2CHO), water, CO_2, and N_2O was observed at higher oxygen coverage which is a partial and total oxidation of propylamine. To learn more about the reaction mechanism of propylamine on oxygen-covered Au(111), and to investigate the effect of oxygen coverage on the production distribution, we conducted a systematic study of selective oxidation of propylamine on Au(111) on different oxygen coverage based on the density functional theory (DFT) calculations, and the calculations are in general agreement with the experimental findings.

Calculations method and models

The calculations were obtained with the Vienna *ab initio* simulation package (VASP) [16]. The exchange-correlation energy and potential were described by generalized gradient approximation (GGA-PW91) [17]. The projector-augment wave (PAW) scheme [18, 19] was employed to describe the interaction between electron-ion. The plane wave set a cut-off energy of 400 eV for the electronic wave functions were expanded. The gold single crystals surface, Au(111), used the lattice constant of 4.18 Å. The periodic four metallic layers slab used a $p(3\times3)$ cell, and was separated by 16 Å of the vacuum region between two successive slabs. For the $p(3\times3)$ cell, two or six oxygen atoms were included in order to model the oxygen coverage of 2/9 and 2/3 ML(Monolayer), respectively. A 3×3×1 Monkhorst-Pack grid was used to perform the Brillouin-zone integrations in the reciprocal space [20]. During the geometry optimization, the top two layers as well as adsorbed species were allowed to be relaxed until the forces were less than 0.05 eV/ Å. Locate the likely transition states by using the general nudged elastic band (NEB) method [21], and lastly the transition state structure optimized must be confirmed by the frequency analysis. The adsorption energy (E_{ads}) is calculated as the following formulas: $E_{ads}= E_{A/O/Au(111)} - E_A - E_{(Au(111)+O)}$, and the activation energy (E_a) based on the equation of $E_a=E_{TS} - E_{IS}$. Here $E_{A/O/Au(111)}$, E_A, $E_{Au(111)}$ and E_O mean the calculated energy of adsorption system, adsorbate, substrate, oxygen atom, respectively. E_{TS} and E_{IS} mean transition state and initial state. ΔH is the reaction heat and can be calculated depending on $\Delta H=E_{FS}-E_{IS}$, here FS is the final state.

Results and discussion

The reaction mechanism of selective oxidation of propylamine on Au(111) was assumed initially by the N-H bond cleavage and followed by the C-H bond break as seen in Scheme 1 [15]. Firstly we study the adsorption of possible species like propylamine on the different model catalysts including Au(111), oxygen covered Au(111) with low oxygen coverage (2/9 ML) and high oxygen coverage (2/3 ML), and then explore the products distribution by activation barrier calculations at low oxygen coverage for partical oxidation of propylamine, and high oxygen coverage for achieving the partial and total oxidation of propylamine to produce CH_3CH_2CHO, H_2O, CO_2, OH, and N_2O.

Adsorption configurations and energies of possible species on Au(111) surface with different oxygen coverage

Our studies aim at the adsorption of propylamine and its dehydrogenated intermediates on Au(111) surfaces using DFT calculation. We built three different but typical adsorption models at the hollow (fcc and hcp), bridge (bri) or top site (top). Figure 1 shows the adsorption of possible species, and the corresponding adsorption energy and geometric parameters are listed in Table 1.

Oxygen atom

As the atomic oxygen is an important reactant in the reaction of propylamine oxidation on the surface, we first study the adsorption of atomic oxygen on Au(111), and the favorable adsorption site which is found to be fcc site. The calculated adsorption energy is −3.26 eV with oxygen coverage of 1/9 ML, −2.96 eV with oxygen coverage of 2/9 ML, and decreasing to −2.51 eV at oxygen coverage of 2/3 ML. The energies and their changing rule with increasing oxygen coverage are almost consistent with the previous DFT results: −3.26 eV (0.11 ML), −3.25 eV (0.25 ML), −2.91 eV (0.50 ML), and −2.45 eV (0.75 ML) calculated by Shi and co-workers [7].

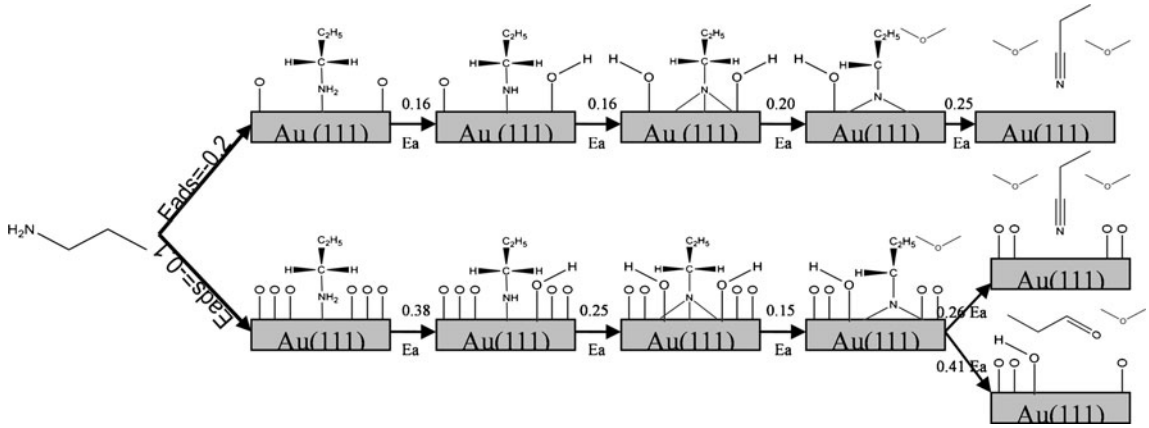

Scheme 1 Reaction mechanism of selective oxidation of propylamine on Au(111) was assumed initially by the N-H bond cleavage and followed by the C-H bond break. Here, all energy unit is electron volts (eV)

$CH_3CH_2CH_2NH_2$

Propylamine ($CH_3CH_2CH_2NH_2$) adsorption is the first step of selective oxidation of propylamine on Au(111) surface. The adsorption site and adsorption energy of propylamine on different oxygen coverage and the related structure parameters are shown in Table 1 and Fig. 1. The most stable site of the propylamine is the top site, no matter how much oxygen is adsorbed to Au(111) surface. For the optimized structure, the N-H bond of propylamine is parallel to the Au (111) surface, while the propyl group($CH_3CH_2CH_2$) have a inclination angle with respect to the surface normal. This is in accord with the calculation results of Hoft et al., in which they found that the angle of phenyl rings and the surface normal is 10° [22]. The C^{α}-N axes are tilted by 43.5°, 49.8°, and 42.2° from the surface normal due to the interaction via the lone pair electrons of nitrogen. As seen from Fig. 1, the distances between the nitrogen atom of the adsorbed propylamine and the gold atom of the Au(111) surface are 2.376 Å on Au(111), 2.383 Å on O/Au(111) (θ_o<0.5) and 2.288 Å on O/Au(111) (θ_o>0.5) surfaces. In our present study, the most stable adsorption site is the top site with adsorption energy of −0.38 eV on Au(111), −0.20 eV on O/Au(111) (θ_o<0.5) and −0.10 eV on O/Au(111) (θ_o>0.5) surfaces. It shows that increasing the oxygen coverage will prevent the adsorption of propylamine. Propylamine weakly adsorbs on the gold surface, which is qualitatively consistent with the experimental results that propylamine desorbed from Au (111) surface at lower temperature (*ca.*140 K). To analyze how oxygen modifies the properties of the gold surface, we turned to calculate the surface d-band center (ε_d), as proposed in the Hammer–Nørskov model [23], in order to characterize surface reactivity as the oxygen pre-covered on surface. As seen in Fig. 2, the calculated d-band centers for the oxygen pre-covered of 2/9 ML and 2/3 ML on Au (111) surface are −3.12 eV and −3.33 eV, which shift toward lower energy compared with -3.05 eV for the Au(111) surface. The DFT calculation show that the metallic Au becomes less active as the oxygen coverage increases, which is in agreement with the adsorption energy trend of propylamine at the top site mentioned above.

To further understand the reason why the surface oxygen affects the adsorption of propylamine, we calculated the projected density of state (PDOS) onto sp orbital of molecular $CH_3CH_7NH_2$ on different oxygen coverage. As seen form Fig. 3, one can find that the DOS at the Fermi lever (or near the Fermi level) is 0.06 states/(eV·atom) on the pure Au (111), and it is increased to 0.71 states/(eV·atom) at the oxygen coverage of 2/9 ML and 2.00 states/(eV·atom) at the oxygen coverage of 2/3 ML. The lower DOS population near the Fermi level means a stable system, so we may conclude that the molecular propylamine becomes more stable on the pure Au(111) surface as compared to the case of oxygen-covered Au(111) system [24].

$CH_3CH_2CH_2NH$

Experimental results showed that the primary step of propylamine decomposition on Au catalysts is the formation of $CH_3CH_2CH_2NH$ species involving the scission of the N-H bond. As shown in Fig. 1, $CH_3CH_2CH_2NH$ is stably adsorbed at the top site on Au(111) formed an N-Au bond. The C^{α}-N axes are tilted by 37.3° (clean), 45.0° (θ_o<0.5), 45.9° (θ_o>0.5) from the surface normal due to the interaction via the lone pair electrons of nitrogen. The N-Au distances are 2.122 Å (clean), 2.099 Å (θ_o<0.5), 2.135 Å (θ_o> 0.5). Moreover, the adsorption energies of $CH_3CH_2CH_2NH$ were found to be −1.21, −0.92, and −0.42 eV at the clean, low oxygen coverage and high oxygen coverage, respectively. With the oxygen coverage increasing from zero to more than 0.5 ML, the adsorption energy becomes low but the tilt angle becomes big.

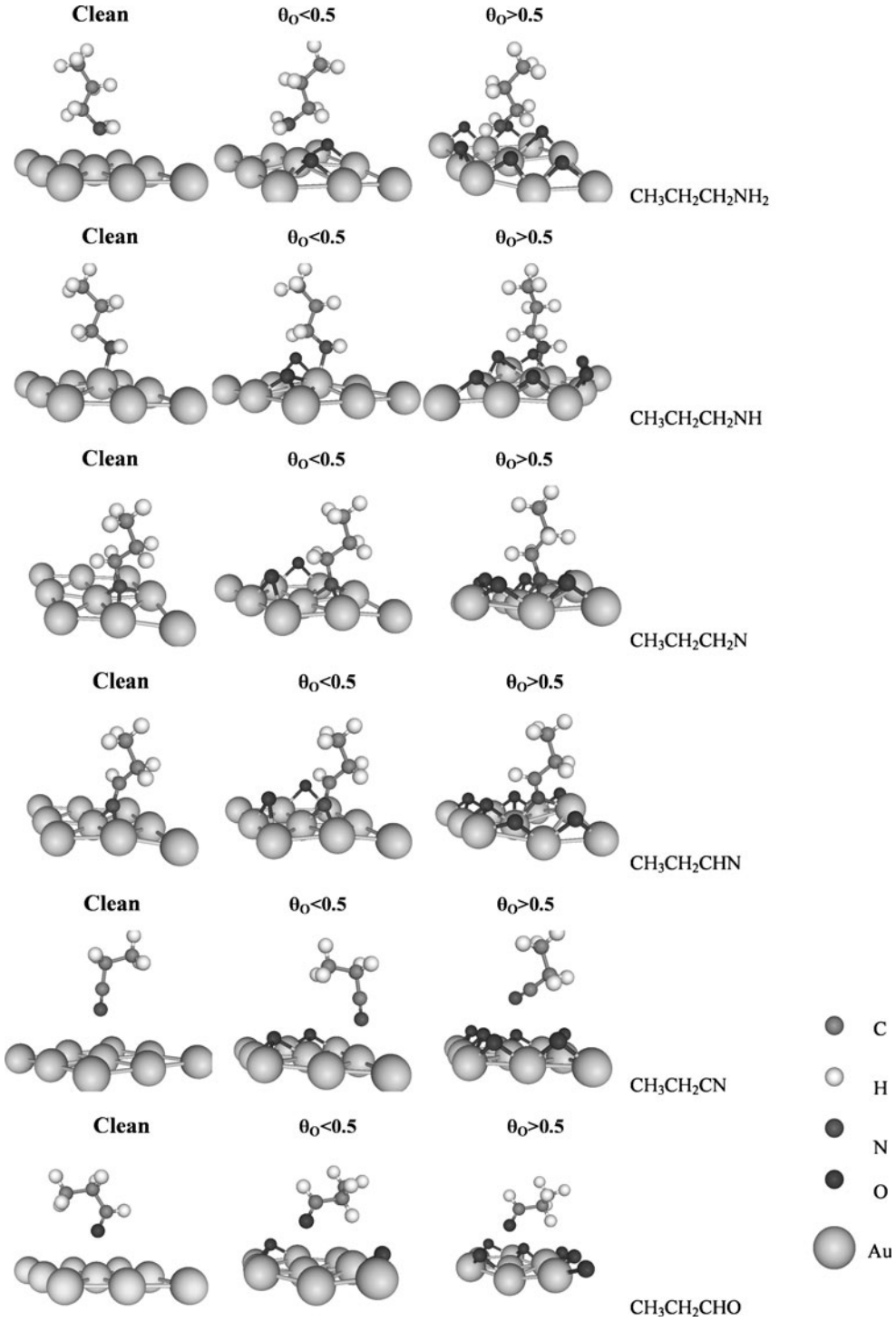

Fig. 1 Optimized geometries of possible species on Au(111) surfaces with different oxygen coverage

$CH_3CH_2CH_2N$

In DFT calculation, $CH_3CH_2CH_2N$ is advanced to the fcc site and formed three N-Au bonds. The optimized results indicated that the $CH_3CH_2CH_2N$ is almost vertical on the surfaces. At clean surface, the distances between N and Au atom are 2.148, 2.143 and 2.137 Å. And the adsorption energy is −2.92 eV. At low oxygen-covered Au(111), the N-Au bond lengths are 2.096, 2.183 and 2.089 Å. The adsorption energy is −2.62 eV. The C^{α}-N axes are tilted by 12.1° (clean), 15.5° (θ_o=2/9 ML) from the surfaces normal due to the interaction via the lone pair electrons of nitrogen. At

Table 1 Adsorption properties (geometric and energetic parameters) of possible species involved in propylamine oxidation on Au(111) surface

	Species	ΔE_{ads}/eV·mol^{-1}	*Site*	$D_{N\text{-}Au}$/Å	$D_{O\text{-}Au}$/Å	Angles[a]/°
Clean/θ_O=0	$CH_3CH_2CH_2NH_2$	−0.38	top	2.376		43.5(C^α-N)
	$CH_3CH_2CH_2NH$	−1.21	top	2.122		37.3(C^α-N)
	$CH_3CH_2CH_2N$	−2.92	fcc	2.148,2.143,2.137		12.1(C^α-N)
	CH_3CH_2CHN	−1.36	bridge	2.157,2.142		27.7(C^α-N)
	CH_3CH_2CN	−0.10	top	2.520		6.9(C^α-N)
	CH_3CH_2CHO	−0.08	top		2.634	26.3(C^α-O)
θ_O<0.5	$CH_3CH_2CH_2NH_2$	−0.20	top	2.383		49.8(C^α-N)
	$CH_3CH_2CH_2NH$	−0.92	top	2.099		45.0(C^α-N)
	$CH_3CH_2CH_2N$	−2.62	fcc	2.096,2.183,2.089		15.5(C^α-N)
	CH_3CH_2CHN	−0.99	bridge	2.085,2.217		26.2(C^α-N)
	CH_3CH_2CN	−0.02	top	2.284		4.7(C^α-N)
	CH_3CH_2CHO	−0.14	top		3.027	28.2(C^α-O)
θ_O>0.5	$CH_3CH_2CH_2NH_2$	−0.10	top	2.288		42.2(C^α-N)
	$CH_3CH_2CH_2NH$	−0.42	top	2.135		45.9(C^α-N)
	$CH_3CH_2CH_2N$	−1.38	fcc	2.188,2.157,2.034		15.9(C^α-N)
	CH_3CH_2CHN	−0.34	bridge	2.055		20.9(C^α-N)
	CH_3CH_2CN	0.00	$\eta^2(C^\alpha,N)$	3.737		67.8(C^α-N)
	CH_3CH_2CHO	−0.01	top		2.960	32.3(C^α-O)

The propylamine ($C^\gamma H_3C^\beta H_2C^\alpha H_2NH_2$) angle to surface normal of the text are shown in the following figure

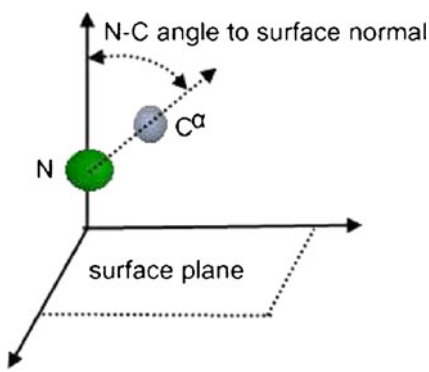

high oxygen-covered Au(111), the C^γ-N axes are the tilt adsorption (15.9°) to the surface with the three N-Au bonds lengths 2.188, 2.157 and 2.034 Å. The adsorption energy is −1.38 eV.

CH_3CH_2CHN

The DFT calculations show that the CH_3CH_2CHN locates at the bridge site formed by two Au atoms. Due to the interaction via the lone pair electrons of nitrogen, the stable site of CH_3CH_2CHN is approximately the bridge site. The N-Au distances are 2.157 and 2.142 Å at clean, 2.085 and 2.217 Å at low oxygen coverage respectively (see Fig. 1) and the length of their N-C bond is 1.278 Å (θ_o=2/9 ML). At the oxygen coverage of 2/3 ML, the N-Au bond is 2.055 Å and the *N*=C bond is 1.262 Å. The calculated results indicated that the adsorption energies are −1.36, −0.99, and −0.34 eV, and the angles of the tilt C^α-N axes with the surfaces are 27.7°, 26.2° and 20.9°on clean, θ_o<0.5 and θ_o>0.5, respectively.

CH_3CH_2CN

Propionitrile (CH_3CH_2CN) is the product of CH_3CH_2CHN dehydrogenation. In calculation, there are two possible models that need to be considered: one mode is the end-on adsorption mode directly on a surface gold, where interaction between the metal and the adsorbate is monodentate; the other mode is the $\eta^2(C^\alpha,N)$ short-bridge adsorption, in which the adsorbate interacts with the surface in a bidentate manner. For the cases of clean Au(11) and 2/9 ML oxygen coverage, the first mode is more stable than the other one. The N-Au distances of propionitrile are 2.520 and 2.284 Å, and the adsorption energies are −0.10 and −0.02 eV on clean

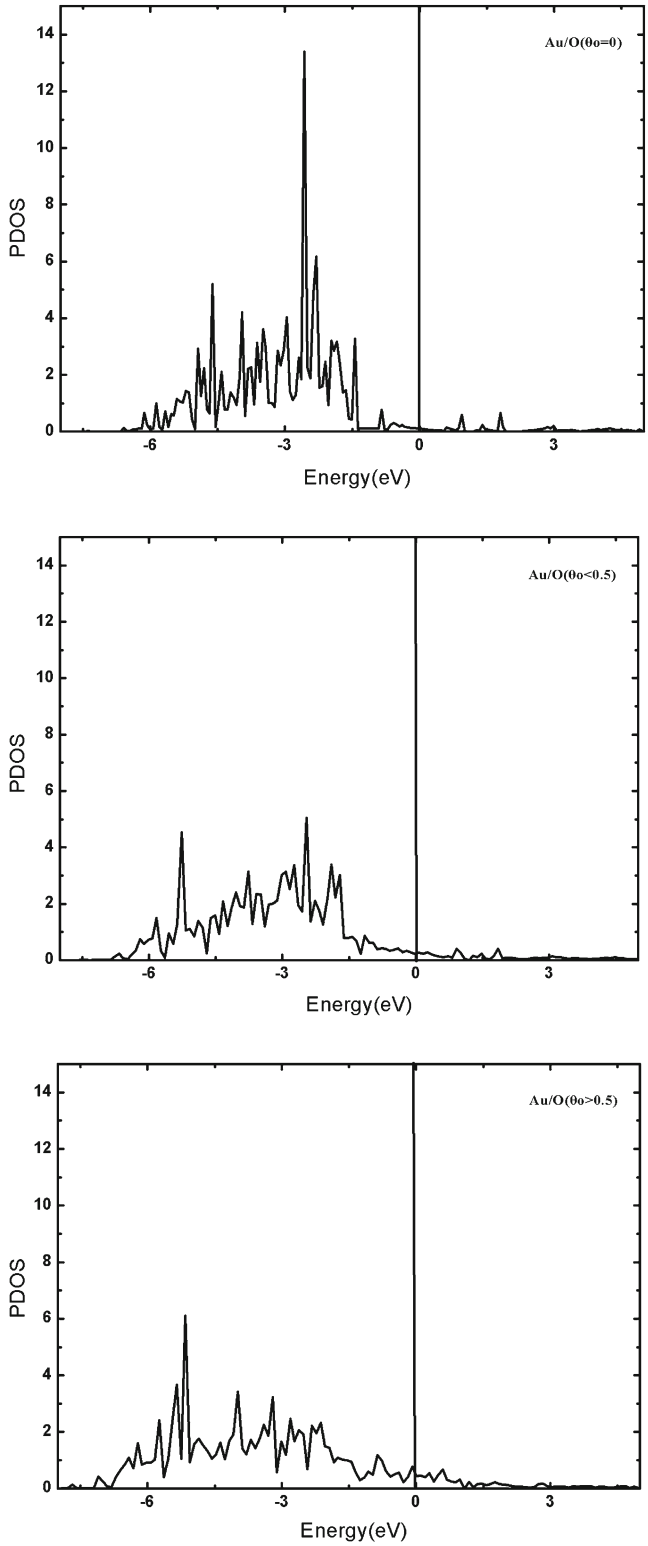

Fig. 2 PDOS of surface gold atom on the Au(111), O/Au(111) (θ_o<0.5), O/Au(111) (θ_o>0.5) surfaces

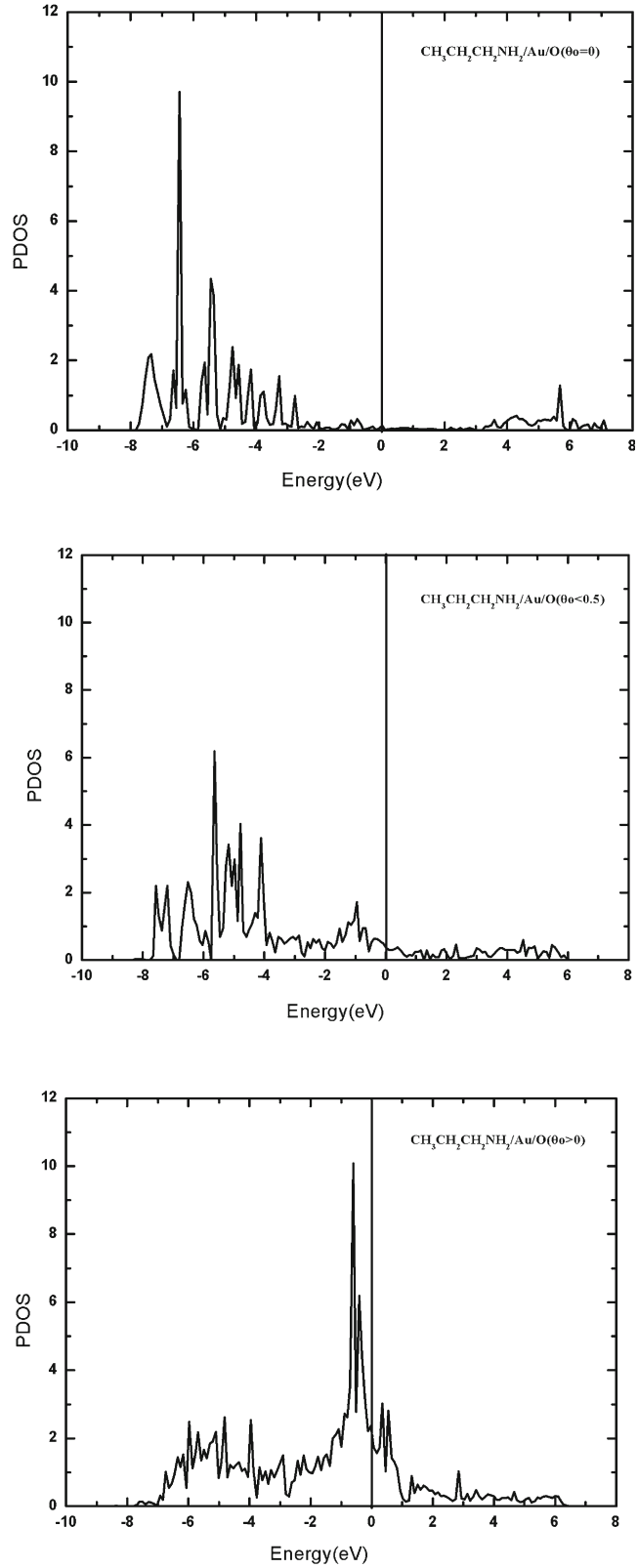

Fig. 3 PDOS of molecular $C_3H_7NH_2$ sp states on the Au(111), O/Au (111) (θ_o<0.5), O/Au(111) (θ_o>0.5) surfaces

and θ_o<0.5, respectively. However, when the oxygen coverage is more than 0.5 ML, the most stable structure is the $\eta^2(C^\alpha,N)$ short-bridge adsorption mode. The distance between N to Au(111) and the angle of $C^\beta C^\alpha N$ respectively is 3.737 Å, 67.8°, and the adsorption energy is nearly zero.

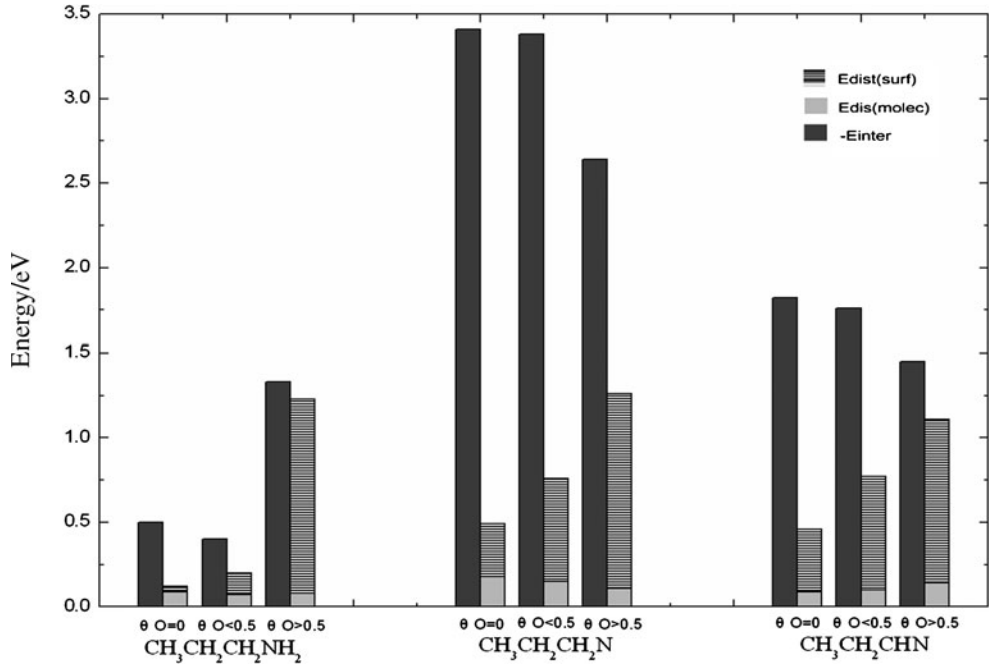

Fig. 4 Decomposition of adsorption energy of $CH_3CH_2CH_2NH_2$, $CH_3CH_2CH_2N$ and CH_3CH_2CHN at different oxygen coverage

Seeing Fig. 1, the angle of propionitrile with respect to the surface normal is much larger at the oxygen coverage of 2/3 ML than at the oxygen coverage of 2/9 ML or Au(111). Due to the very small adsorption energies, the propionitrile is easily desorbed from the Au-based catalysts.

CH_3CH_2CHO

The partial oxidation of CH_3CH_2CHN can produce propionaldehyde (CH_3CH_2CHO) only at high oxygen coverage. The DFT calculation show that the most stable adsorption site of propionaldehyde is the top site on both clean and high/low oxygen-covered Au(111) with its oxygen atom close to substrate. On clean and oxygen–covered Au(111) surfaces, the C^{α}-O axes have the angles (26.3°, 28.2°, 32.3°) with respect to the surfaces normal line, and with the O-Au distances of 2.634, 3.027, 2.960 Å. The adsorption energies are −0.08, −0.14, −0.01 eV on clean and oxygen–covered Au(111), respectively.

Based on the above DFT calculations, one may conclude that the adsorption energy of all the species related to increasing oxygen coverage, and the d-band center of metallic Au away from the Fermi level may be responsible for such a trend.

We may analyze the reason of the adsorption energy change, by the binding interaction to the metal (E_{inter}), and the distortion of the molecule and the metal as compared with its gas-phase state (E_{dist}) [25, 26] which have opposite contributions. The former can strengthen a stability, but the later can cause distortion of molecule and metal surface, causing destabilization of the system [27]. This can be expressed by an equation:

$$E_{ads} = E_{dist(molec)} + E_{dist(surf)} + E_{inter}. \quad (1)$$

These terms are listed for $CH_3CH_2CH_2NH_2$, $CH_3CH_2CH_2N$ and CH_3CH_2CHN on the Au(111), O/Au (111) (θ_o<0.5), O/Au(111) (θ_o>0.5) in Fig. 4. The $E_{dist(molec)}$ of the three species are 0.09, 0.18, 0.09 eV on the Au(111), 0.07, 0.15, 0.10 eV on O/Au(111) (θ_o<0.5) and 0.08, 0.11, 0.14 eV on O/Au(111) (θ_o>0.5). So it is observed that the $E_{dist(molec)}$ for all the adsorbed species is almost the same and small on the different surfaces. On the contrary, the distortion of the surfaces is very serious in the order of Au (111)<O/Au(111) (θ_o<0.5)<O/Au(111) (θ_o>0.5). Especially, at oxygen coverage of 2/3 ML, $E_{dist(sur)}$ is larger than that at the Au(111). As the oxygen coverage increases on the Au surface, the interaction of the surface and molecule becomes large. However, with the oxygen coverage increasing, the change of the interaction between the surface and the oxygen atom is lower than the transformation of $E_{dist(molec)}+E_{dist(surf)}$, and thus the substrate deformation may play a dominant role to reduce the adsorption energy. So with the oxygen coverage from 2/9 ML to 2/3 M/L, as the $E_{dist(surf)}$ increases (Fig. 3) the adsorption system becomes less stable.

The reaction of propylamine at different oxygen coverage

After getting the most stable configurations of reactant and selective oxidation intermediates as well as the products, and we can gain the reaction mechanism by the kinetics study. From the experimental results we know the maximal reaction temperature of propylamine on oxygen-covered Au (111) is ~330 K, and one can deduce the highest barrier for the elemental step is ~0.80 eV if the pre-exponential factor for the first order reaction was estimated to be ~10^{13} based on the transition state theory [28]. The energy barrier and

reaction heat for each step are given in Table 2, and the Figs. 5 and 6 display the possible structure of reactant, transition state and final products at low and high oxygen coverage.

Reaction of propylamine oxidation at low oxygen coverage

The first step of propylamine on oxygen-covered Au(111) may be processed via the N-H bond broken or the C-H bond broken (i.e., path a_1 or path a_2 as seen in Fig. 5). Though path a1, $CH_3CH_2CH_2NH$ and OH are formed by the oxidative dehydrogenation process of the propylamine molecule. In the TS, the H fragment has already dissociated from $CH_3CH_2CH_2NH$ and moves close to the pre-adsorbed O atom. The calculated activation barrier is 0.16 eV. In an analogous way, propylamine dissociation along path a_2 on O/Au(111) associates to a C-H breaking process and the formation of $CH_3CH_2CHNH_2$ and HO. The barrier for this step is 0.60 eV. Obviously, the channel via the N-H bond cleavage is easier than that of C-H bond broken and thus we study the reaction mechanism initiated by the N-H bond cleavage in the following section. After the formation of $CH_3CH_2CH_2NH$, and then it would dehydrogenation to produce $CH_3CH_2CH_2N$ in the presence of chemisorbed oxygen (path b as seen in Fig. 5). In path b, with the dehydrogenation of $CH_3CH_2CH_2NH$ to $CH_3CH_2CH_2N$, the hydrogen atom abstracted from the rest of N-H bond reacts with adsorbed oxygen to form O-H bond. The energy barrier of this step is 0.16 eV and the related reaction heat is −0.35 eV. During the reaction process, at the transition state, the N-H bond length is 1.245 Å, the O-H bond length is 1.236 Å, and the distance between N atom and the surface Au atom is ca. 2.13 Å. In path c, CH_3CH_2CHN and H_2O are produced by the cleavage of C-H bond of $CH_3CH_2CH_2N$ by the reaction with the chemisorbed OH. The energy barrier is 0.20 eV and the corresponding reaction heat is −1.53 eV. In the final step, CH_3CH_2CHN is further oxidized to CH_3CH_2CN by the help of adsorbed OH, in which an energy barrier and reaction heat are 0.25 and −1.61 eV, respectively. When propionitrile and water are co-adsorption on the on Au(111) surface, it was found that the propionitrile is tilted by 38.8° with respect to the surface normal due to the interaction with water on the O/Au(111) surface. To conclude, the above calculation results suggested that the N-H bond broken is the favored reaction path, and followed by the C-H bond broken by the aid of chemisorbed O and /or OH species. The final products of propylamine at low oxygen coverage are propionitrile and water. Moreover, it was found the energy barriers are generally small (smaller than 0.50 eV), which means these reactions can be carried out at room temperature. In fact, the experimental results showed that the propionitrile can be produced at 280 K [15].

Reaction of propylamine oxidation at high oxygen coverage

On Au(111) surface of high oxygen coverage, the co-adsorption site of $CH_3CH_2CH_2NH_2$ (top) and O (fcc) were found to be the most stable system. The calculated possible reaction paths are displayed in Fig. 6. Similar to the situation of low oxygen coverage as discussed above, the calculation results indicated that the barrier of N-H bond cleavage involved in $CH_3CH_2CH_2NH_2$ is 0.38 eV (path a_1 as seen in Fig. 6), which is smaller than that of C-H bond cleavage (0.50 eV of path a_2 as seen in Fig. 6). So the N-H bond broken is the first step on higher oxygen coverage. Following path a1, $CH_3CH_2CH_2NH$ can further dehydrogenation to form $CH_3CH_2CH_2N$ by the aid of oxygen atom adsorbed on Au(111) (path b). In path b, the product ($CH_3CH_2CH_2N$) is chemisorbed to the fcc site with the nitrogen. The distance between the nitrogen atom of the adsorbed $CH_3CH_2CH_2N$ and the three gold atom of the Au(111) surface is 2.16, 2.13, and 2.07 Å, which is close with that of the adsorbed $CH_3CH_2CH_2N$ (2.13, 2.14, and 2.12 Å) at low oxygen

Table 2 Activation energy (Ea) and structures of transition state of propylamine on different oxygen coverage pre-adsorbed Au(111) surface (energy unit in eV and bond length in Å)

		E_a/eV	ΔH/eV	D(N–H)/Å	D(O–H)/Å	D(C–H)/Å	D(C-N)/Å	D(C–O)/Å
$\theta_O<0.5$	path a_1	0.16	0.10	1.188	1.311	–	–	–
	path a_2	0.60	−0.86	–	1.400	1.291	–	–
	path b	0.16	−0.35	1.245	1.236	–	–	–
	path c	0.20	−1.53	–	1.475	1.236	–	–
	path d	0.25	−1.61	–	1.350	1.284	–	–
$\theta_O>0.5$	path a_1	0.38	0.34	1.294	1.195	–	–	–
	path a_2	0.50	−2.59	–	1.499	1.208	–	–
	path b	0.25	−0.84	1.299	1.153	–	–	–
	path c	0.15	−2.69	–	1.746	1.177	–	–
	path d	0.26	−2.84	–	1.485	1.236	–	–
	path e	0.41	−2.83	–	–	–	1.271	2.920

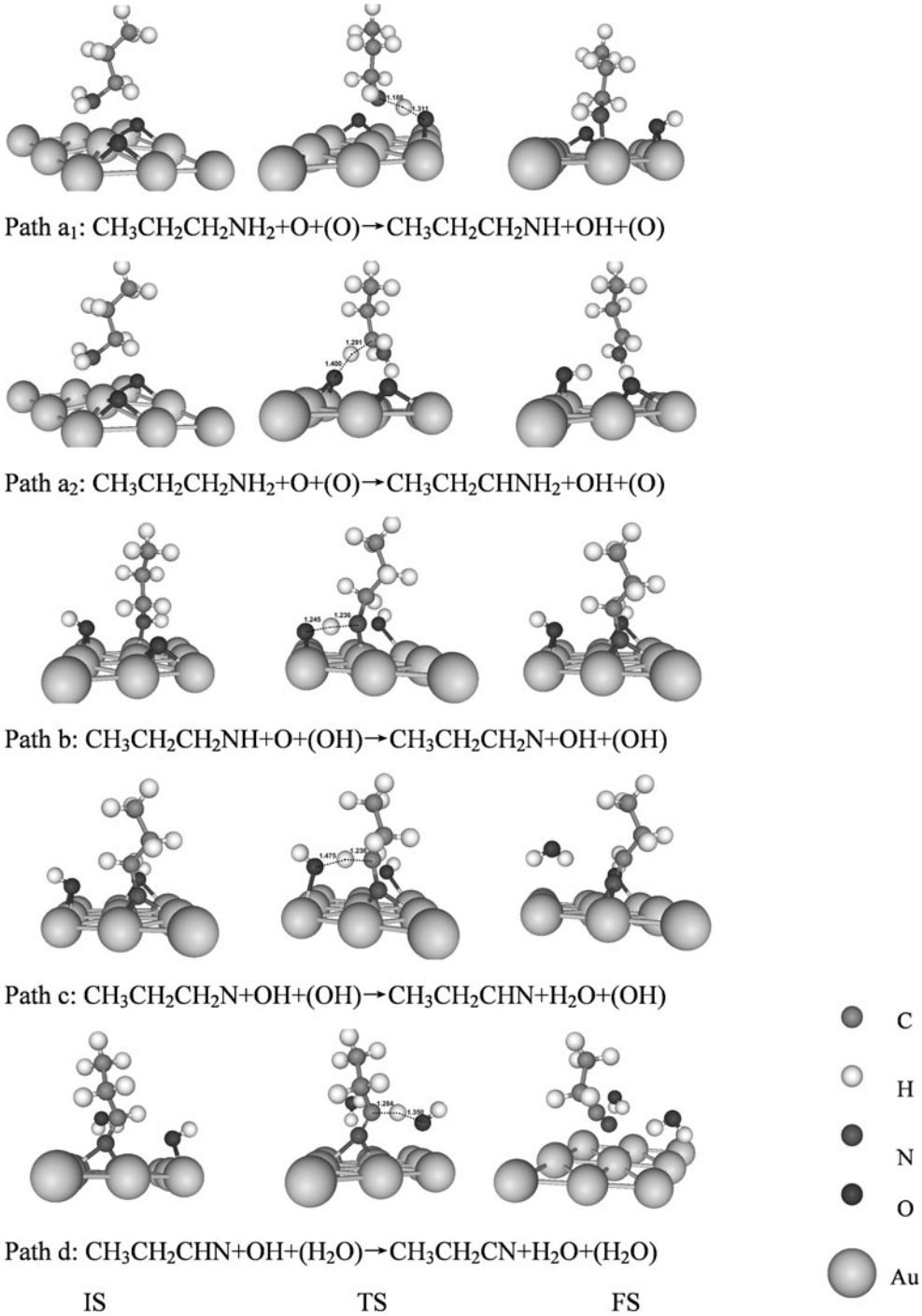

Fig. 5 Snapshots of propylamine oxidation at low oxygen covered Au(111). The IS, TS, and FS mean the initial state, transition state and final state, respectively

coverage. In both path a_1 and path b, both OH as products adsorbed in bridge site. Once $CH_3CH_2CH_2N$ formed, it can be further oxidized to CH_3CH_2CHN by the help of OH with an energy barrier of 0.15 eV (path c). After the formation of CH_3CH_2CHN, it can either react with the OH species to produce CH_3CH_2CN and H_2O by the cleavage of C-H bond (path d), or react with chemisorbed oxygen to produce CH_3CH_2CHO and N atom by the cleavage of C-N bond (path e). For these two steps, the energy barriers are 0.26 and 0.41 eV, and the reaction heats are −2.84 and −2.83 eV for C-H bond broken and C-N bond broken, respectively. Due to the effect of OH and H_2O, the adsorption site of CH_3CH_2CN, CH_3CH_2CHO is tilted 33.7°, 61.8° to the surface, which are very different from our calculation without OH and H_2O (shown in Fig. 1).

Comparing between low and high oxygen coverages, one can find that the energy barrier at the high oxygen coverage is generally larger than that at low oxygen coverage, this is

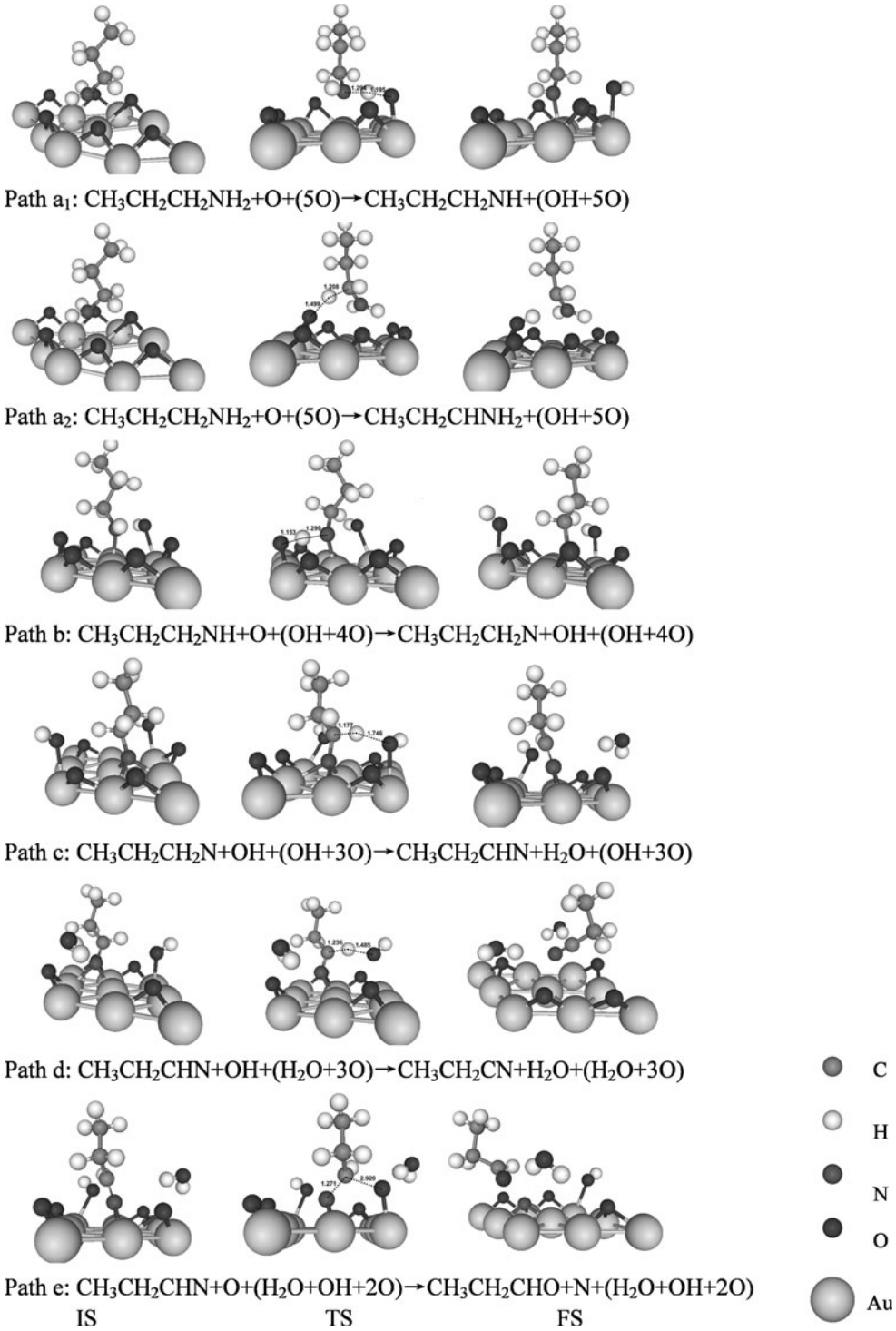

Fig. 6 Snapshots of propylamine oxidation at high oxygen covered Au(111). The IS, TS, and FS mean the initial state, transition state and final state, respectively

consistent with the experimental findings that the propylamine can be dehydrogenated into propionitrile at ~280 K through the broken of N-H and C-H bond at low/high oxygen coverage, and the main product of the reaction are propionaldehyde and water at 310 K at high oxygen coverage [15]. The reasons why the barrier on higher oxygen coverage is larger than that on lower oxygen coverage are due to the following two factors: one is the more oxygen atoms on the Au(111) will block the active site for further reaction, and the other one is the metallic Au becomes less active due to the presence of oxygen atom (this can be confirmed by the d-band center calculation as mentioned above).

In order to gain the dominant factors controlling the changes in the reaction barrier on different oxygen coverage, we analyze the energy barrier for the first step ($CH_3CH_2CH_2NH_2 \rightarrow CH_3CH_2CH_2NH+H$) by the scheme

proposed by Hammer [29]. The formula used to analyze the physical nature of reaction barrier when the reaction begins from $CH_3CH_2CH_2NH_2$ molecular in the gas phase is:

$$E_{act} = E^{TS}_{CH_3CH_2CH_2NH} + E^{TS}_{H} + E^{int}_{CH_3CH_2CH_2NH\cdots H} + \Delta E^{def}_{CH_3CH_2CH_2NH_2} - E^{IS}_{CH_3CH_2CH_2NH_2} + \Delta E_{sub.} \quad (2)$$

The value ($E^{TS}_{CH_3CH_2CH_2NH} + E^{TS}_{H}$) decreases from −0.80 ($\theta_o$=2/9 ML) to −3.71 ($\theta_o$=2/3 ML) eV, and $E^{int}_{CH_3CH_2CH_2NH\cdots H}$ changed from −1.19 eV on low oxygen coverage to 1.28 eV on high oxygen coverage. The adsorption energy of the IS configuration ($CH_3CH_2CH_2NH_2$), $E^{IS}_{CH_3CH_2CH_2NH_2}$, is −0.10 eV. The deformation energy of substrate (ΔE_{sub})(*i.e.,* 0.72 eV on θ_o=2/9 ML and 1.65 eV on θ_o=2/3 ML) implies that the substrate in the TS becomes more deformed with the increasing oxygen on surface. However, the molecule deformation energy ($\Delta E^{def}_{CH_3CH_2CH_2NH_2}$=$E^{gas}_{CH_3CH_2CH_2NH\cdots H}$−$E^{gas}_{CH_3CH_2CH_2NH_2}$), measures the effect of the structural deformation of $CH_3CH_2CH_2NH_2$ on the barrier, which can be ignored for similar values on both oxygen-covered Au(111) (namely 1.23 and 1.06 eV on θ_o=2/9 ML and θ_o=2/3 ML, respectively). Since the energy barrier increases with increasing of oxygen coverage, and thus we may conclude that the deformation energy of substrate maybe a crucial factor for controlling the barrier because its variation trend is the same as the energy barrier. In fact, this is consistent with our above analysis for the original of adsorption energy that the deformation energy of substrate caused by the presence of chemisorbed oxygen plays the key role controlling the trend of binding energy.

Conclusions

The reaction mechanism for the propylamine selective oxidation on oxygen-covered gold has been studied by the density functional theory calculation with the periodic slab model. It shows that the oxygen on gold surface can activate propylamine to produce propionitrile and propionaldehyde. The present DFT calculations show that the adsorption energies of the species become lower at the higher oxygen coverage. In addition, the present results also show that the coverage of surface oxygen also plays a key role in the determination of production distribution. At lower-oxygen-coverage, the propylamine undergoes dehydrogenation to produce H_2O and CH_2CH_3CN. At high oxygen coverage, propylamine can be partial oxidated, yielding propionitrile, propionaldehyde and water. In general, the activation energy of the low oxygen coverage is less than the high oxygen coverage. At low oxygen coverage the breaking of N-H, C-H bond and production of propionitrile are easier than at high oxygen coverage.

Acknowledgments This work was supported by the National Natural Science Foundation of China (Grants No. 20273034, 20673063) and the Tianhe-1 supercomputer in Tianjin.

References

1. David H (1991) Great lakes environmentalists push for zero chemical pollution. Chem Eng News 69:12–14. doi:10.1021/cen-v069n011.p012
2. Florig HK (1997) Peer Reviewed: China's Air Pollution Risks. Environ Sci Technol 31:274A–279A. doi:10.1021/es972315t
3. Gong JL, Ojifinni RA, Kim TS, White JM, Mullins CB (2006) Selective Catalytic Oxidation of Ammonia to Nitrogen on Atomic Oxygen Precovered Au(111). J Am Chem Soc 128:9012–9013. doi:10.1021/ja062624w
4. Lopez N, Garcia-Mota M, Gomez-Diaz J (2008) NH3 oxidation on oxygen-precovered Au(111): A density functional theory study on selectivity. J Phys Chem C 112:247–252. doi:10.1021/jp077205f
5. Gardin DE, Somorjai GA (1992) Vibrational spectra and thermal decomposition of methylamine and ethylamine on Ni(111). J Phys Chem 96:9424–9431. doi:10.1021/j100202a067
6. Carley AF, Davies PR, Edwards D, Jones RV, Parsons M (2005) Molecularly resolved studies of the reaction of pyridine and dimethylamine with oxygen at a Cu(110) surface. Top Catal 36:21–32. doi:10.1007/s11244-005-7859-1
7. Shi HQ, Stampfl C (2007) First-principles investigations of the structure and stability of oxygen adsorption and surface oxide formation at Au(111). Phys Rev B 76:075327. doi:10.1103/PhysRevB.76.075327
8. Liu XY, Madix RJ, Friend CM (2008) Unraveling molecular transformations on surfaces: a critical comparison of oxidation reactions on coinage metals. Chem Soc Rev 37:2243–2261. doi:10.1039/B800309M
9. Min BK, Friend CM (2007) Heterogeneous gold-based catalysis for green chemistry: low-temperature CO oxidation and propene oxidation. Chem Rev 107:2709–2724. doi:10.1021/cr050954d
10. Deng XY, Baker TA, Friend CM (2006) A pathway for NH addition to styrene promoted by gold. Angew Chem Int Ed 45:7075–7078. doi:10.1002/anie.200602876
11. Haruta M (1997) Size-and support-dependency in the catalysis of gold. Catal Today 36:153–166. doi:10.1016/S0920-5861(96)00208-8
12. Corti CW, Holliday RJ, Thompson DT (2005) Commercial aspects of gold catalysis. Appl Catal A: Gen 291:253–261. doi:10.1016/j.apcata.2005.01.051
13. Caballero C, Valencia J, Barrera MA, Gil A (2010) Selective hydrogenation of citral over gold nanoparticles on alumina. Powder Technol 203:412–414. doi:10.1016/j.powtec.2010.04.029
14. Deng XY, Friend CM (2008) Selectivity switch for nitrogen functionalization of styrene on Au(111). Surf Sci 602:1066–1071. doi:10.1016/j.susc.2008.01.002
15. Gong JL, Yan T, Mullins CB (2009) Selective oxidation of propylamine to propionitrile and propionaldehyde on oxygen-covered gold. Chem Commun :761–763 doi:10.1039/B821050K
16. Kresse G, Furthmüller J (1996) Efficiency of ab-initio total energy calculations for metals and semiconductors using a plane-wave basis set. Comput Mater Sci 6:15–50. doi:10.1016/0927-0256(96)00008-0
17. Kresse G, Hafner J (1993) *Ab initio* molecular dynamics for liquid metals. Phys Rev B 47:558–561. doi:10.1103/PhysRevB.47.558
18. Blochl PE (1994) Projector augmented-wave method. Phys Rev B 50:17953–17979. doi:10.1103/PhysRevB.50.17953

19. Kresse G, Joubert D (1999) From ultrasoft pseudopotentials to the projector augmented-wave method. Phys Rev B 59:1758–1775. doi:10.1103/PhysRevB.59.1758
20. Monkhorst HJ, Pack JD (1976) Special points for brillouin zone integrations. Phys Rev B 13:5188–5192. doi:10.1103/PhysRevB.13.5188
21. Henkelman G, Uberuaga B, Jonsson HJ (2000) A climbing-image NEB method for finding saddle points and minimum energy paths. J Chem Phys 113:9901–9904. doi:10.1063/1.1329672
22. Hoft RC, Ford MJ, McDonagh AM, Cortie MB (2007) Adsorption of amine compounds on the Au(111) surface: a density study. J Phys Chem C 111:13886–13891. doi:10.1021/jp072494t
23. Hammer B, Morikawa Y, Nørskov JK (1996) CO chemisorption at metal surfaces and overlayers. Phys Rev Lett 76:2141–2144. doi:10.1103/PhysRevLett.76.2141
24. Feibelman PJ, Hamann DR (1984) Electronic structure of a "Poisoned" transition-metal surface. Phys Rev Lett 52:61–64. doi:10.1103/PhysRevLett.52.61
25. Morin C, Simon D, Sautet P (2006) Intermediates in the hydrogenation of benzene to cyclohexene on Pt(111) and Pd(111): a comparison from DFT calculations. Surf Sci 600:1339–1350. doi:10.1016/j.susc.2006.01.033
26. Santarossa G, Iannuzzi M, Vargas A, Baiker A (2008) Adsorption of naphthalene and quinoline on Pt, Pd and Rh: A DFT study. Chem Phys Chem 9:401–413. doi:10.1002/cphc.200700534
27. Morin C, Simon D, Sautet P (2004) Chemisorption of benzene on Pt(111), Pd(111) and Rh(111) metal surfaces: a structural and vibrational comparison from first principles. J Phys Chem B 108:5653–5665. doi:10.1021/jp0373503
28. Dumesic JA, Rudd DF, Aparicio LM, Rekoske JE (1993) The microkinetics of heterogeneous catalysis. American Chemical Society, Washington DC, p 40
29. Hammer B (2000) Adsorption, diffusion, and dissociation of NO, N and O on flat and stepped Ru(0001). Surf Sci 459:323–348. doi:10.1016/S0039-6028(00)00467-2